Laminar Natural Convection Heat Transfer in an Air Filled Square Cavity with Two Insulated Baffles Attached to its Horizontal Walls *

Himsar AMBARITA†, Kouki KISHINAMI†, Mashasi DAIMARUYA†, Takeo SAITOH‡, Hiroshi TAKAHASHI†, and Jun SUZUKI†

Abstract

This paper attempts to study numerically a differentially heated square cavity, which is formed by horizontal adiabatic walls and vertical isothermal walls. Two perfectly insulated baffles were attached to its horizontal walls at symmetric position. Heat transfer by natural convection of dry air was studied by solving mass, momentum and energy equations numerically. Streamlines and isotherms are produced and heat transfer is calculated. A parametric study is carried out using following parameters: Rayleigh number from 10^4 to 10^8, non-dimensional thin baffles length are 0.6, 0.7, and 0.8, non-dimensional baffle positions S_b from 0.2 to 0.8. It was observed that the two baffles trap some fluid in the cavity and affect the flow fields. The flow for cavities with S_b <0.5 at low *Ra* tends to circulate as a primary vortex strangled by the baffles while at high *Ra* it tends to separate into two different vortexes. For the cavities with S_b >0.5 it tends to separate into two different vortexes at low *Ra* while at high *Ra* tends to circulate as a primary vortex strangled by the baffles. It is found that Nusselt number is an increasing function of *Ra*, a decreasing one of baffle length, and strongly depends on S_b. Another interesting phenomenon of the typical cavity is that a particular case is the opposite of the other case as long as the sum of S_b is equal to 1. Thus, the typical cavity can allow the heat flow in one direction but significantly blocks it in the opposite direction. The typical cavity can be proposed as a heat version of a diode. The heat may be transferred up to 42% from one direction but blocked up to 98% in the opposite direction by using a particular cavity with L_b =0.7 and S_b=0.4 at Ra=10^8.

Key Words: *Cavity with baffles, Natural convection, Heat version of diode*

Nomenclature

g	:	Gravitational acceleration	[m/s^2]
H	:	Cavity height	[m]
k	:	Thermal conductivity	[W/(m·K)]
K	:	Heat flow coefficient defined in Eq. (3)	
l	:	Baffle length	[m]
L	:	Non-dimensional baffle length, $=l/H$	
Nu	:	Nusselt number defined in Eq. (10)	
p	:	Pressure	[Pa]
P	:	Non-dimensional pressure	
Pr	:	Prandtl number, $=\upsilon/\alpha$	
Ra	:	Rayleigh number, $=g\beta(T_h-T_c)H^3/\alpha\nu$	
s	:	Baffle position	[m]
S	:	Non-dimensional baffle position, $=s/H$	
T	:	Temperature	[K]
U,V	:	Non-dimensional velocities	
α	:	Thermal diffusivity	[m^2/s]
β	:	Coefficient of thermal expansion	[K^{-1}]
θ	:	Non-dimensional temperature	
υ	:	Kinematic viscosity	[m^2/s]
ρ	:	Density	[kg/m^3]
ψ	:	Stream function	

Sub/Superscripts

b	:	related to baffle
c	:	related to cold surface
h	:	related to hot surface
l	:	related to left vertical wall
r	:	related to right vertical wall
-	:	average

1 Introduction

Natural convection in an air filled cavity with vertical walls that are heated and cooled while its horizontal walls are adiabatic has received a great consideration because many of the industrial applications

* Received: February 27, 2006, Editor: Mamoru SENDA

† Department of Mechanical System Engineering, Muroran Institute of Technology (27-1 Mizumoto cho, Muroran 050-8585, JAPAN)

‡ School of Environmental Studies, Tohoku University (01 Aoba-yama, Sendai 980-8579 JAPAN)

employ this concept as a prototype. Noticeable examples include heating and ventilating of rooms, solar collector systems, electronic cooling devices, and cooling of nuclear reactors. In many applications, for some reasons, the cavity is partitioned by attaching baffle(s) to its vertical and (or) to its horizontal wall(s). Recently, studies of heat transfer and fluid flow characteristics of the partitioned cavity has come under scrutiny both numerically and experimentally [1-17]. Based on the baffle(s) position, the published works can be segregated into two groups. The baffle(s) are attached to the vertical wall(s) [1-11] and the baffle(s) are attached to the horizontal wall(s) [12-17] of the cavity. Since this paper considers a square cavity with a baffle attached to each of its horizontal walls, only the typical problems will be briefly reviewed.

The cavity with baffle(s) attached to its horizontal walls received less attention than the cavity with baffle(s) attached to its vertical wall(s). After an extensive literature study, we have found three publications about this particular cavity. Bajorek and Llyod [14] studied experimentally a differentially heated air filled square partitioned cavity for Rayleigh numbers $1.25\times10^5 - 2.16\times10^6$. The insulated baffle is attached to the horizontal walls at positions in the middle. Non-dimensional baffle length is 0.25. The effect of the baffle positions was not considered. It was found that the baffles significantly influence the heat transfer rate and the average Nusselt numbers reduced to approximately 15 % compared to the non-partitioned cavity. Observations of the interferometric fringes indicated that the core region is unsteady beginning at Rayleigh numbers 3.5×10^5 . Jetli et al. [15] studied numerically a differentially heated air filled square partitioned cavity for Rayleigh numbers $10^4 - 3.55\times10^5$ with three different combinations of the baffle positions. The first case, the bottom baffle is on the hot side and the top baffle is on the cold side, the second case both baffles are in the middle, and the third case the bottom baffle is on the cold side and the top baffle is on the hot side. Non-dimensional baffles length is fixed at 0.33. The results clearly demonstrate that the baffles positions have a significant effect on the heat transfer and flow characteristics of the fluid. For all baffles locations, the average Nusselt number is smaller than the corresponding value in a cavity without baffle.

Recently, Bilgen [16] studied numerically the differentially heated air filled partitioned shallow cavity (aspect ratio 0.3 to 0.4) for Rayleigh number from 10^4 to 10^{11}. Non-dimensional baffle length was varied from 0 to 0.15. The baffle position was varied in the middle or slightly farther away from the heated side (non-dimensional positions are 0.5-0.6) and its conductivity is 20 relative to the air conductivity (for usual construction materials). It was found that the flow regime was laminar for Rayleigh numbers up to 10^8 thereafter turbulent. The heat transfer was reduced when two baffles were used instead of one, aspect ratio was made smaller, and positions of the baffles were farther away from the hot wall.

The literature review cited above shows that the study of a partitioned cavity with non-dimensional baffle's length more than 0.5 have not been reported. It was reported that the length of the baffle strongly affects the heat transfer and flow characteristics in the cavity but no trapped fluid phenomenon was captured.

In this paper we present a numerical study of natural convection in an air filled partitioned square cavity. The cavity was differentially heated and to its top and its bottom walls a baffle was attached. The baffles are thin, perfectly insulated and non-dimensional length of more than 0.5 in order to capture the trapped fluid. The positions of the top baffle from the right wall and the bottom baffle from the left wall are the same, so the configuration of the baffles in the cavity is always symmetrical. The literature review shows that this problem has not been addressed [22]. The objective of this paper is to make clear the effects of the long baffles on the flow and temperature fields and on the heat transfer characteristics of the cavity. The result can be expected from this paper is to show that the cavity with baffles are attached to its horizontal walls can be proposed as a heat version of diode which allows the heat to flow in one direction but significantly blocks it in the opposite direction.

2 Problem Definition

The typical cavity with the boundaries and its coordinates system are depicted in Figure 1. In this study only the square cavity is considered, its height and width are denoted by H . The cavity is differentially heated, left and right walls are isothermal at T_h and T_c respectively $(T_h > T_c)$ and horizontal walls are adiabatic. Two thin baffles with non-dimensional length L_b , perfectly insulated, were attached to the top and the bottom wall. The non-dimensional position of the bottom baffle from the left wall and top baffle from the right wall are the same and denoted by S_b .

The flow is assumed to be two-dimensional and in steady state condition. The compressibility, radiation heat exchange, and dissipations are negligible. All of the thermal properties are constant, except density in the buoyancy force. Boussinesq approximation is used to model the buoyancy force. The governing equations are converted into the non-dimensional form by defining the non-dimensional variables.

$$X = \frac{x}{H}\ ,\quad Y = \frac{y}{H}\ ,\quad U = \frac{uH}{\alpha}\ ,\quad V = \frac{vH}{\alpha}\ ,\quad P = \frac{pH^2}{\rho\alpha^2}\ ,$$

$$\theta = \frac{T - T_c}{T_h - T_c} \tag{1}$$

The pressure p in the above equation is the reduced pressure which is defined as local pressure subtracted by hydrostatic pressure. Based on these non-dimensional

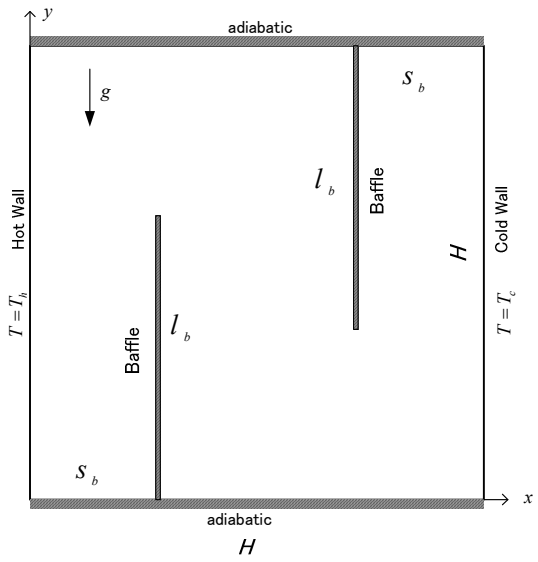

Fig. 1 Schematic of the square cavity with thin insulated baffles attached to the horizontal walls

variables, the governing equations are obtained as follows.

$$\frac{\partial U}{\partial X}+\frac{\partial V}{\partial Y}=0 \tag{2}$$

$$U\frac{\partial U}{\partial X}+V\frac{\partial U}{\partial Y}=-\frac{\partial P}{\partial X}+Pr\left(\frac{\partial^2 U}{\partial X^2}+\frac{\partial^2 U}{\partial Y^2}\right) \tag{3}$$

$$U\frac{\partial V}{\partial X}+V\frac{\partial V}{\partial Y}=-\frac{\partial P}{\partial Y}+Pr\left(\frac{\partial^2 V}{\partial X^2}+\frac{\partial^2 V}{\partial Y^2}\right)+Ra\,Pr\,\theta \tag{4}$$

$$U\frac{\partial \theta}{\partial X}+V\frac{\partial \theta}{\partial Y}=\left(\frac{\partial^2 \theta}{\partial X^2}+\frac{\partial^2 \theta}{\partial Y^2}\right) \tag{5}$$

The boundary conditions are:

On the left wall: $U=V=0,\ \ \theta=1$ (6)

On the right wall: $U=V=0,\ \ \theta=0$ (7)

On the top and bottom walls: $U=V=0,\ \ \dfrac{\partial\theta}{\partial Y}=0$ (8)

On the baffles: $U=V=0$ (9)

In order to compare total heat transfer rate, Nusselt number is used. The local and average Nusselt numbers are defined as follows.

$$Nu_y=-\frac{\partial\theta/\partial X\big|_{X=0}}{(\theta_h-\theta_c)} \tag{10}$$

$$\overline{Nu}=\int_0^1 Nu_y\,dY \tag{11}$$

The comparison parameter for flow characteristic is represented by the stream function, and defined as follow.

$$U=-\frac{\partial\psi}{\partial Y},\ \ V=\frac{\partial\psi}{\partial X} \tag{12}$$

3 Numerical Procedure

All of the governing equations were transformed into sets of algebraic equations based on the finite volume method. The staggered grid system was used. In order to handle convective and diffusion terms the power law scheme was employed. The sets of algebraic equations were solved by using the line by line method which is combined with the Thomas algorithm. The SIMPLE algorithm [21] was used to couple the velocity, pressure, and temperature fields.

In the SIMPLE algorithm under-relaxation factor is an essential problem and there is no special rule in determining the proper under-relaxation factor. A large under-relaxation factor, especially for momentum equations, will lead the calculation into divergence however a very small under-relaxation factor leads to a lengthy calculation. After some calculations, employing an under-relaxation factor larger than 0.2 for momentum equations (especially for cases *Ra* higher then 10^6) will not reach the convergence. In order to get the convergence for all problems, the small under-relaxation factors were employed. Considering both computational cost and convergence the under-relaxation factor for momentum equations is 0.01, for pressure it is 0.2, and for temperature it is 0.8. Based on this procedure the FORTRAN codes to solve all of the governing equations have been developed.

3.1 Grid Independence Test

In this study, non-uniform grid spacing was employed. However near the walls and the baffles even smaller grid spacing was used. In order to determine the proper grid numbers due to accuracy and computational time, a grid independence test was conducted for a particular case. Four different grid sizes were tested in the case where L_b=0.6 and S_b=0.3. $\overline{Nu}$ and the maximum absolute stream function are used as the sensitivity measure of the accuracy of the solution, the results are presented in Table 1.

Table 1 Comparison parameters for grid sensitive test

Grid numbers	$\overline{Nu}$	$\lvert\psi\rvert_{\max}$	$\Delta\overline{Nu}$ (%)	$\Delta\lvert\psi\rvert_{\max}$ (%)
60×60	0.7543	8.51	7.75	1.88
80×80	0.8128	8.67	3.81	0.91
100×100	0.8438	8.749	1.11	0.39
120×120	0.8532	8.783	-	-

Comparison of the both parameters values among four different cases suggest that two grids sizes 100×100 and 120×120 give nearly the same results (deviation less than 1.5 %). Considering both the accuracy and the computational time, the 100×100 grid size was employed for all calculations.

3.2 Validation of the Code

In order to make sure that the developed codes are free of error coding, a validation test was conducted. Calculations for an air filled square cavity without baffle for Ra=10^4 to 10^8 were carried out and the results are shown in Table 2. The results of the previous publications for the same problem are also presented in the table. Data from the table shows that the results of the code, even though there are some differences, do agree very well with the previous works results. Those differences are not essential, the maximum difference is 1.7 %, and probably caused by the different grids sizes and round-offs in the computational process. Based on this successful validation, the problem is solved by using the code.

Table 2 Comparison of the present result and the previous works result

Reference	Average Nusselt numbers, $\overline{Nu}$				
	Ra=10^4	Ra=10^5	Ra=10^6	Ra=10^7	Ra=10^8
Davish[18]	2.234	4.51	8.798	-	-
Hortmann [19]	2.4468	5.5231	8.8359	-	-
Saitoh[20]	2.2415	-	8.7126	-	-
Collins[3]	2.244	4.5236	8.8554	-	-
Nag[2]	2.24	4.51	8.82	-	-
Shi[1]	2.247	4.532	8.893	16.935	-
Bilgen[7]	2.245	4.521	8.8	16.629	31.520
Present	2.228	4.514	8.804	16.52	30.48

Flow and temperature fields for the square cavity without baffle are presented in Fig. 2 for reference. Fig. 2(a) shows the isotherms. As natural convection strengthened, temperature contours show slight deviation from the pure conduction case with the isotherms becoming skewed. Under high Rayleigh numbers conditions, the degree of distortion from the pure conduction case is very marked and the contour lines become almost horizontal lines around the center of the cavity. Fig. 2(b) shows the streamlines. The rise of the fluid due to heating on the left wall and consequent falling of the fluid on the right wall creates a clockwise rotating vortex, referred to as the primary vortex.

Another feature of these streamline patterns is that the streamlines become more packed next to the side wall as the Rayleigh number increases. This suggests that the flow moves faster as natural convection is intensified. The maximum absolute value of the stream function in the cavity is also shown in Fig. 2. Therefore, the maximum absolute value of the stream function can be viewed as a measure of the intensity of natural convection in the cavity. As the Rayleigh number increases the maximum absolute value of the stream function increases. This means the intensity of natural convection in the cavity increases as the Rayleigh number increases.

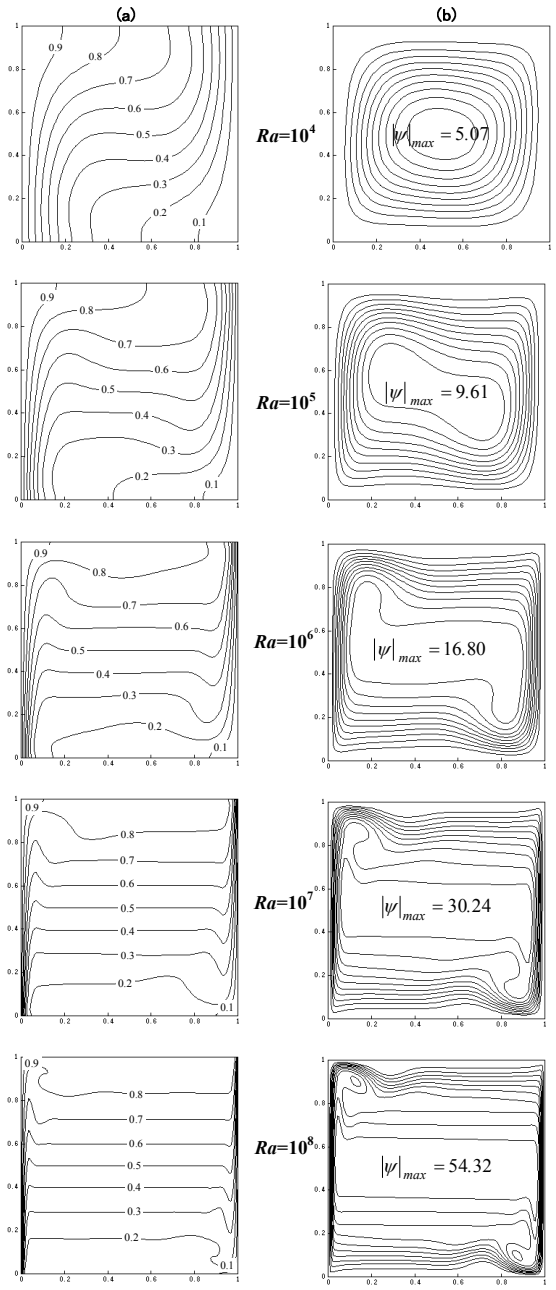

Fig. 2 Isotherms (a) and streamlines (b) of natural convection in a square cavity without baffle

4 Results and Discussion

In order to understand the flow and temperature fields and heat transfer characteristics of the typical cavity a total of 90 cases were considered. To study the effects of the baffle position, the non-dimensional baffle positions S_b= 0.2, 0.3, 0.4, 0.6, 0.7, and 0.8 were considered. To study the effects of baffle length, the non-dimensional baffle lengths L_b=0.6, 0.7, and 0.8 were considered. The fluid inside the cavity is dry air with Pr = 0.7 and Rayleigh number varied from 10^4 to 10^8. Flow and temperature fields and Nusselt number are examined.

4.1 Flow and Temperature Fields

Flow fields for the typical cases with non-dimensional baffle length $L_b = 0.6$ are presented in Fig. 3. The plots are arranged going from left to right with the ascending of Rayleigh numbers and from top to bottom with the ascending of S_b values. The maximum value of the absolute stream function for each case is also presented in the figure. We note that for all *Ra* the appearance of the flow fields and maximum value of the absolute stream function in all cases is totally different to the square cavity without baffle. This is already expected because the presence of the two baffles with L_b more than 0.5 inside the cavity totally modifies the flow field patterns. A glance at Fig. 3 shows that the flow fields can be divided into two different patterns. The first pattern is the fluid circulates and creates a large clockwise primary vortex strangled by the baffles. The second pattern is the fluid separated into two different vortexes. The two baffles create fluid trapping phenomena in the cavity.

The first row of Fig. 3 is the flow fields for the case when $S_b = 0.2$. Since $S_b < 0.5$, the bottom baffle is on the hot side and the top baffle is on the cold side of the cavity. At a low Rayleigh number $Ra=10^4$ there are two trapped fluids in the cavity, hot trapped fluid and cold trapped fluid. The hot trapped fluid exists between the bottom baffle and the hot wall and the cold trapped fluid between the top baffle and cold wall. This is because at $Ra=10^4$ natural convection is too weak to make the trapped fluids moving and also the space of the trapped fluids is limited due to a small S_b.

The natural convection creates a primary vortex strangled by these two trapped fluids. For $Ra=10^5$ as intensity of natural convection increases, some of the trapped fluids are flowing and the primary vortex starts dividing into two vortexes. For $Ra=10^6$ natural convection is strong enough to make all of the trapped fluids flowing.

In order to satisfy the continuity, the circulation on the hot side is separated from the circulation on the cold side. The primary vortex has been divided into two different vortexes, cold vortex and hot vortex. These two vortexes are separated by one trapped fluid which is stagnant between the two baffles. For cases with $Ra=10^7$ and $Ra=10^8$ the trapped fluid can be seen clearly. This is because the vortex on each side becomes more vigorous showed by the more packed streamlines.

The second row of Fig. 3 is the flow fields when $S_b=0.3$. The figure shows that even for a low Rayleigh number $Ra=10^4$ the primary vortex starts dividing into two vortexes. When $Ra=10^5$ is reached the primary vortex has been divided into two different vortexes. This is because the space between each baffle and the nearest vertical wall is larger compared to the corresponding cases when $S_b=0.2$. For Rayleigh numbers higher than 10^5 each vortex becomes more vigorous and the trapped fluid between the two baffles can be seen clearly. The effects of the S_b value can be seen clearly by observing the case with $S_b=0.4$. In this case even for a low Rayleigh number $Ra=10^4$ the primary vortex has been divided into two separated vortexes. This is because the spaces between each baffle and the nearest vertical wall are larger than the latter cases.

The forth row until the sixth row of the Fig. 3 are the cases when $S_b > 0.5$. In these cases the bottom baffle is on the cold side and the top baffle is on the hot side of the cavity. The flow fields for case with $S_b = 0.6$ are shown in the forth line of the figure. At $Ra=10^4$ and $Ra=10^5$ there are two vortexes in the cavity and a trapped fluid exists between the two baffles. This is because at the low *Ra,* the strength of the flowing fluids is not strong enough to penetrate the stagnant fluid between the two baffles. Since the spaces between each baffle and the nearest vertical wall are wide enough for the flowing fluid the circulations in both sides, cold side and hot side, are not mixed.

For $Ra=10^6$ the fluid moves faster as the Rayleigh number increases, the two vortexes penetrate the stagnant fluid then merge to become a primary vortex. The natural convection can not move all of the fluid in the entire cavity and some of the fluids are trapped in the hot side and the cold side. The hot trapped exists between the top baffle and the hot wall. While the cold trapped fluid exists between the bottom baffle and the cold wall. The primary vortex circulates in a single cell strangled by these two trapped fluids.

At higher Rayleigh numbers $Ra=10^7$ and $Ra=10^8$ the fluid moves faster, indicated by the contour of the stream line more packed, and make the trapped fluids more clear. The fifth and sixth rows of the Fig. 3 are flow field for cases with $S_b = 0.7$ and $S_b = 0.8$ respectively. The figure shows that even for $Ra=10^4$ the flow field has become a primary vortex strangled by two trapped fluids. This is because the space of each trapped fluid is smaller compared to the case with $S_b = 0.6$.

Similar observations were made (not shown) for cases with $L_b = 0.7$ and $L_b = 0.8$. In these cases the flow fields show the same pattern with the corresponding case with $L_b = 0.6$.

Temperature fields when $L_b = 0.6$ are presented in Fig. 4. The plots are arranged going from left to right with the ascending of the Rayleigh number and from top to bottom with the ascending of the S_b value. The contour level increments for each case are kept constant at 0.1. Indeed in comparison to the square cavity without baffles the appearance of the temperature fields is strongly modified due to the presence of the two insulated baffles.

The first row of Fig. 4 is for $S_b = 0.2$. At $Ra=10^4$ when the natural convection is weak the isotherms take place only in the areas where the fluid moves. The isotherms show slight deviations from the pure conduction case with the contour lines becoming skewed. In the trapped fluid areas heat transfer is inactive due to presence of the insulated baffles and stagnant fluids.

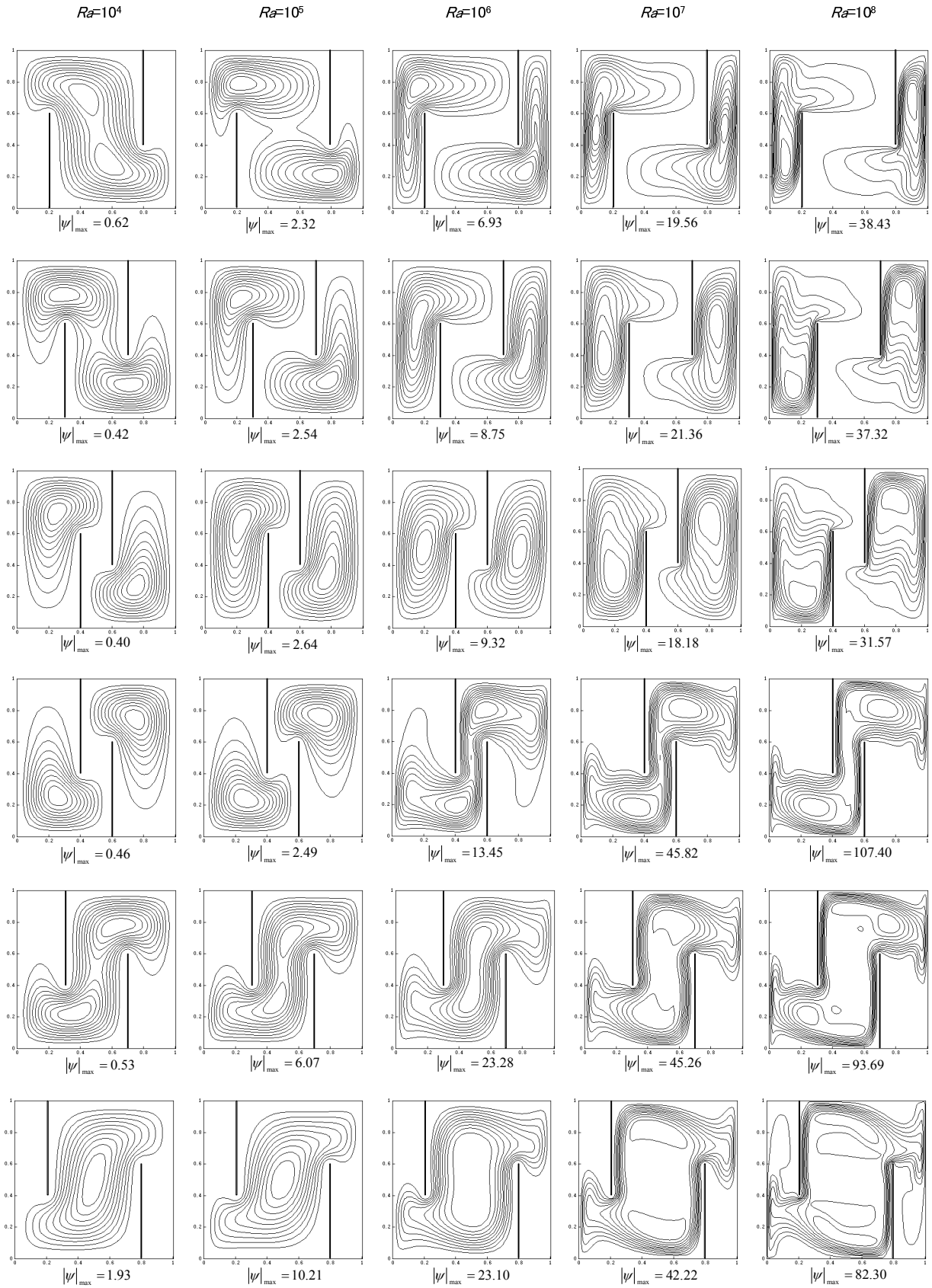

Fig. 3 Streamlines for $L_b = 0.6$: the first column: Ra=10^4, second: Ra=10^5, third: Ra=10^6, fourth: Ra=10^7, fifth: Ra=10^8. The first row: $S_b = 0.2$, second: $S_b = 0.3$, third: $S_b = 0.4$, fourth: $S_b = 0.6$, fifth: $S_b = 0.7$, sixth: $S_b = 0.8$

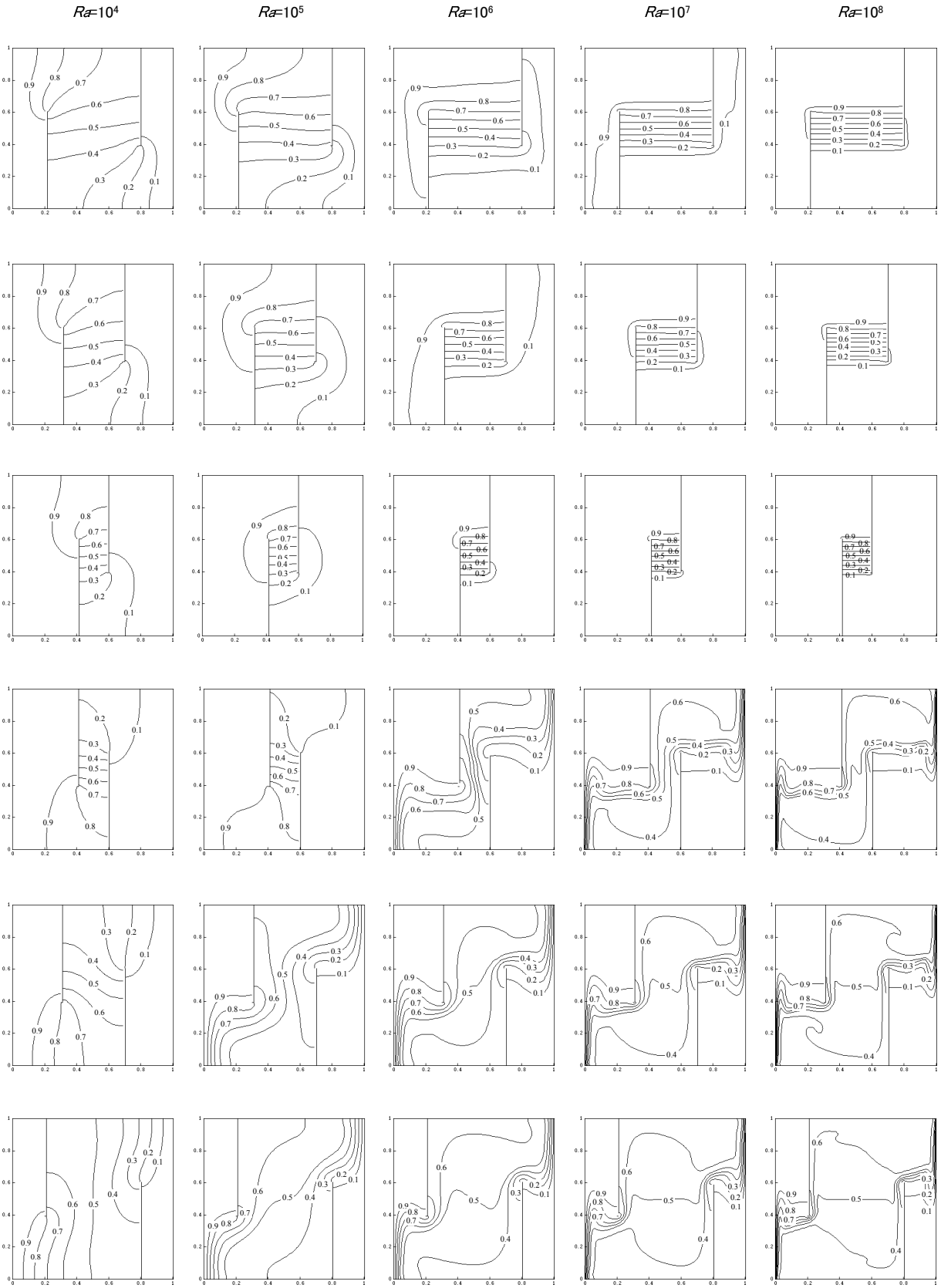

Fig. 4 Temperature fields for $L_b = 0.6$: the first column: Ra=10^4, second: Ra=10^5, third: Ra=10^6, the fourth: Ra=10^7, fifth: Ra=10^8. The first row: $S_b = 0.2$, second: $S_b = 0.3$, third: $S_b = 0.4$, fourth: $S_b = 0.6$, fifth: $S_b = 0.7$, sixth: $S_b = 0.8$

At Ra=10^5 the isotherms in the top left and bottom right of the cavity become more skewed but almost horizontal between the two baffles. This is because natural convection is more vigorous in the top left and bottom right of the cavity but becomes weak between the two baffles due to separation of the primary vortex. For Ra=10^6, we note that the primary vortex has separated completely. Isotherms diminished on vortex areas but were more packed on the trapped fluid between the baffles. This is due to temperature difference on the vortex areas is small due to fluid circulation but it is high on the trapped fluid. For high Rayleigh numbers Ra=10^7 and Ra=10^8 the isotherms become more packed in the trapped fluid area but almost disappeared on the vortex areas. This is due to the vortexes becoming more vigorous and results in a very small temperature difference. The temperature difference on the vortex areas is only about 0.2 for Ra=10^7 and is only about 0.1 for Ra=10^8. The trapped fluid blocks the convection heat transfer from the hot wall to the cold wall and conduction heat transfer is only considered. The second row and the third row of Fig. 4 are the temperature fields for cases when baffle positions $S_b = 0.3$ and $S_b = 0.4$. The figure shows that the appearance of the temperature fields of these cases is similar to the cases when $S_b = 0.2$.

The fourth row is for case when $S_b = 0.6$. At Ra=10^4 where the flow is still separated into two vortexes and a trapped fluid exists between the two baffles the isotherms are skewed on the vortex areas but almost horizontal in the trapped fluid area. At Ra=10^5 the isotherms are more skewed in the vortex areas but less horizontal in the trapped fluid area since intensity of the natural convection increases. At Ra=10^6 when the two vortexes have merged the isotherms are totally modified. The trapped fluids in the top left and bottom right of the cavity are inactive with respect to convective and conductive heat transfer due to the presence of stagnant fluid and insulated baffles, in Fig. 4 showed by the empty isotherms areas. These trapped fluids reduce the end-to-end heat transfer on the vertical walls. The isotherms show that the natural convection takes places only on uncovered area of the vertical walls. For higher Rayleigh numbers Ra=10^7 and Ra=10^8 natural convection becomes more vigorous and the fluid moves faster and the isotherms become more packed next to uncovered vertical walls. The fifth and the sixth rows of Fig. 4 are the temperature fields for cases when the baffle positions $S_b = 0.7$ and $S_b = 0.8$. The figure shows that the appearance of the temperature fields of the latter cases are quite similar with the corresponding case when $S_b = 0.6$. Similar observations were also made (not shown) for $L_b = 0.7$ and $L_b = 0.8$, which show the similarity with the corresponding cases when $L_b = 0.6$.

4.2 Heat Transfer

In order to evaluate how the presence of the two baffles affects the heat transfer rate through the cavity, the average Nusselt number will be discussed. The average Nusselt numbers for all cases as a function of Rayleigh number, Ra and for various parameters, $L_b = 0.6$, $L_b = 0.7$, and $L_b = 0.8$ are presented in Fig. 5, Fig. 6, and Fig. 7 respectively. In the figures $\overline{Nu}$ for the cavity without baffle is also presented by a dashed line as a reference. Generally, as expected $\overline{Nu}$ is an increasing function of Ra and a decreasing function of L_b. The figures show that the appearance of the $\overline{Nu}$ lines for cases when $S_b < 0.5$ is totally different from $S_b > 0.5$. Nusselt numbers for cases when $S_b < 0.5$ are lower than the cases when $S_b > 0.5$ especially at high Ra regions. This is because in these cases, the trapped fluid between the two baffles totally blocks the convective heat transfer. However for the cases with $S_b > 0.5$, total heat transfer rate correlates with the natural convection on uncovered vertical walls. There is an exception, in the case when $S_b = 0.6$ is different from the cases $S_b = 0.7$ and $S_b = 0.8$ at low Ra regions. This is because in these regions the circulation is still separated by the trapped fluid.

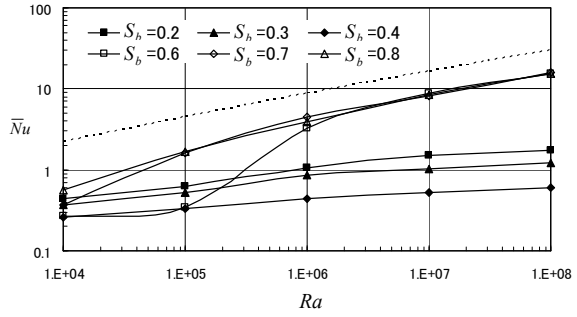

Fig. 5 Nusselt number as a function of Ra for the case $L_b = 0.6$ with S_b as a parameter

Fig. 5 shows the case with L_b=0.6. For $S_b = 0.2$, $\overline{Nu}$ is decreased by 80% at Ra=10^4 and is 94.2% at Ra=10^8, the average is 87.9%. At low Ra, the circulation is not perfectly separated and causes a relatively lower decrease compared to the higher Ra. For S_b=0.3, $\overline{Nu}$ is decreased by 83% at Ra=10^4 and is 96% at Ra=10^8, the average is 90.5%. These values suggest that the case with S_b=0.3 blocks the heat transfer rate more effectively than the case with S_b=0.2. Indeed since S_b < 0.5 $\overline{Nu}$ correlates with conduction heat transfer through the trapped fluid. Thus $\overline{Nu}$ is trapped fluid's dimension dependent that increases as its width increases but decreases as its length increases. Moving the baffles from $S_b = 0.2$ to $S_b = 0.3$ will reduce the width of the trapped fluid from 0.6 to 0.4 and causes $\overline{Nu}$ to decreases. At a high Ra where the two vortexes are vigorous, related to small temperature difference on the vortex

areas, the ratio $\overline{Nu}$ will almost be the same as the ratio of trapped fluid's width. For example at Ra=10^8 $\overline{Nu}$ =1.76 for S_b=0.2 and =1.21 for S_b=0.3, the ratio is 1.46, while the width ratio is 0.6/0.4=1.5. Furthermore, for $S_b = 0.4$ where the width of the trapped fluid becomes smaller, equal to 0.2, $\overline{Nu}$ is decreased by 88% at Ra=10^4 and is 98% at Ra=10^8, the average is 94.2%. These values suggest that the case with $S_b = 0.4$ blocks the heat transfer rate more effectively than the latter cases. This is because the width of the trapped fluid becomes smaller. The width ratio of the trapped fluid for $S_b = 0.3$ and $S_b = 0.4$ is 0.4/0.2=2, this ratio is almost the same with $\overline{Nu}$ ratio that is 1.91 for Ra=10^6, 1.97 for Ra=10^7 and 2.0 for Ra=10^8. These results reveal that the change in $\overline{Nu}$ is trapped fluid's width dependent which is related to the baffle positions.

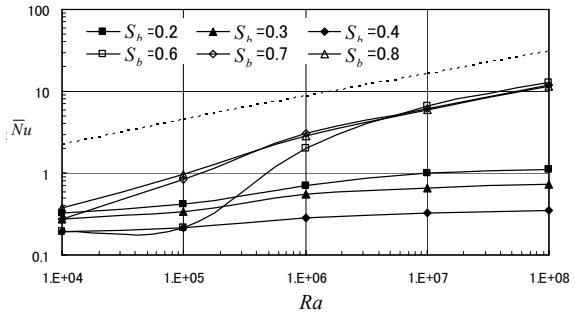

Fig. 6 Nusselt number as a function of Ra for the case $L_b = 0.7$ with S_b as a parameter

For S_b=0.6, $\overline{Nu}$ is decreased by 88% at Ra=10^4, 92% at Ra=10^5, 63% for Ra=10^6, and less than 50% for Ra>10^6. At low Ra regions this case blocks the heat transfer significantly (>85%) because the two vortexes have not merged. For Ra>10^6 the heat transfer rate is blocked less than 50% because the two separated vortexes have merged. For S_b=0.7, $\overline{Nu}$ is decreased by 83% at Ra=10^4, 63% at Ra=10^5, less than 50% for Ra>10^5. And for S_b=0.8, $\overline{Nu}$ is decreased by 74% at Ra=10^4, 62% at Ra=10^5, about 50% for Ra>10^5. These results are in accordance with the observations that are made in Fig. 3 and Fig. 4 that the trapped fluid in the top left and bottom right of the cavity cover some vertical walls and inactive respect to convection and conduction heat transfer. The uncovered vertical walls still have a significant effect on the total heat transfer rate.

The graph also shows that for cases when $S_b > 0.5$ at high Ra regions $\overline{Nu}$ is only a function of Ra and it is not affected by the baffle positions. This is because total heat transfer rate correlates with the uncovered vertical walls only. Another feature is that at high Ra regions the lines of $\overline{Nu}$ for the cases are parallel with the cavity without baffle. This is because at high Ra regions the heat transfer characteristics for these cases will be similar in comparison to the cavity without baffle. The only difference is in the length of the uncovered vertical walls

Fig. 6 is for L_b=0.6. The graph shows that the appearance of $\overline{Nu}$ lines pattern is similar with the corresponding case when $L_b = 0.6$. The only differences are in the quantity of $\overline{Nu}$. This is because the length of the baffles changes dimension of the trapped fluid and finally affects the quantity of $\overline{Nu}$. For cases with S_b < 0.5 where $\overline{Nu}$ depends on the dimension of the trapped fluid between the two baffles, the longer baffles are related to the longer trapped fluid. The length of the trapped fluid for the case with $L_b = 0.6$ is 0.2 and for the case with L_b=0.7 is 0.4, the ratio is 0.5. Since $\overline{Nu}$ is trapped fluid's dimension dependent that increases as its width increases but decreases as its length increases, $\overline{Nu}$ for L_b=0.7 is about 0.5 times lower than L_b=0.6. For cases with $S_b > 0.5$ where the total heat transfer rate correlates with the natural convection on the uncovered vertical walls, the baffles length show significant effect in the quantity of $\overline{Nu}$. The baffle with L_b=0.7 covers the vertical wall 70% (the uncovered wall is 30%). Since the heat transfer rate correlates with natural convection on the uncovered vertical walls then the cases with longer uncovered areas reveal the higher $\overline{Nu}$. This results in $\overline{Nu}$ for case with L_b=0.7 being lower than L_b=0.6.

Fig. 7 is for $L_b = 0.8$. It was observed, again, that the appearance of the $\overline{Nu}$ lines is similar to the latter cases $L_b = 0.6$ and $L_b = 0.7$. As expected since the baffles are longer than in the latter cases the total heat transfer rate for this case is lower. The figure shows Nusselt numbers for cases with $S_b < 0.5$ always less than 1 and for cases with $S_b > 0.5$ always less than 10. The reasons are already discussed in the aforementioned paragraph.

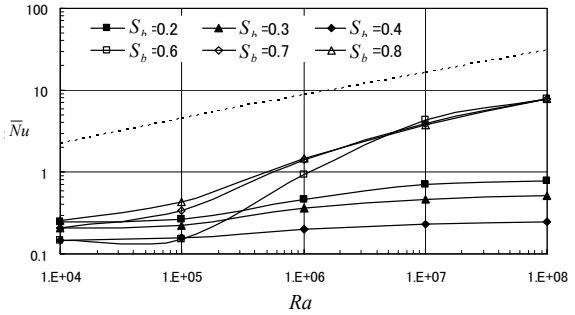

Fig. 7 Nusselt numbers as a function of Ra for the case $L_b = 0.8$ with S_b as a parameter

4.3 Heat Version of Diode

Another interesting phenomenon of the typical cavity is that a particular case is the opposite of the other case as long as the sum of S_b is equal to 1. The case when S_b=0.2 is the opposite of the case when S_b=0.8,

the case when S_b=0.3 and S_b=0.7, and the case when S_b=0.4 and S_b=0.6. For example, a pair S_b=0.3 and S_b=0.7, the case when S_b=0.3 will reveal the same results (flow fields, temperature fields and $\overline{Nu}$) with S_b=0.7 if its vertical walls temperature are reversed with each other. In this cavity ($S_b = 0.3$), if the left wall is hotter than the right wall $\overline{Nu}$ at Ra=10^8 is 1.21 (blocks the heat 96%) but if the right wall is hotter than the left wall (the same case with S_b=0.7) $\overline{Nu}$ at Ra=10^8 is 15.9 (passes the heat 52.3%) compared to the cavity without baffle. This means that the same cavity can significantly block the heat from the left to the right wall but can also allow it to flow from the right to the left wall.

An additional calculation for a particular cavity with $S_b = 0.3$ and $L_b = 0.6$ at Ra=10^7 when $\theta_l = 1$ was carried out. The right wall was fixed at temperature $\theta = 0$ and the left wall temperature was varied from $\theta_l = 1$, 0.8, 0.5, 0.2, -0.2, -0.5, -0.8, and -1.

The flow fields are presented in Fig. 8. The figure shows that for $\theta_l = 1$, 0.8, 0.5, and 0.2 the trapped fluid exists between the two baffles, separates the primary vortex and switches off the convective heat transfer. This results in a very low $\overline{Nu}$ or blocks the heat transfer significantly. For $\theta_l = -0.2$, -0.5, -0.8, -1 the separated vortexes have been merging and create a counter clockwise primary vortex. The fluids in the bottom left and top right of the cavity become trapped due to presence of the baffles and inactive respect to convective and conductive heat transfer. The heat transfer rate is still significant due to natural convection on the uncovered vertical walls.

Nusselt number for this particular case as a function of the left wall temperature is shown in Fig. 9. As a reference, we note that $\overline{Nu}$ =16.75 for the cavity without baffle. The figure shows that if the temperature of the left wall is hotter than the right wall $\overline{Nu}$ is very low and only about 1 (the heat is blocked up to 94%). If the temperature of the left wall is colder than the right wall $\overline{Nu}$ is 8.23 (the heat is transferred up to 49%). In order to evaluate the performance of the cavity to transfer and to block the heat flow a parameter has been promoted and named as a *heat flow coefficient*. The *heat flow coefficient* is defined as a ratio of $\overline{Nu}$ when the fluid flow creates a primary vortex and $\overline{Nu}$ when it is blocked. The *heat flow coefficient* is calculated by using equation (13).

$$K = \frac{\overline{Nu}_{circulating}}{\overline{Nu}_{blocked}} \tag{13}$$

By using this equation the *heat flow coefficient* for the particular cavity with $S_b = 0.3$ and $L_b = 0.6$ at Ra=10^7 is K=8.23/1=8.23. It does mean that the particular cavity can pass the heat 8.23 times more than the blocked heat.

The *heat flow coefficient* for all cases at Ra=10^6, Ra=10^7, and Ra=10^8 are presented in Fig. 10. The figure

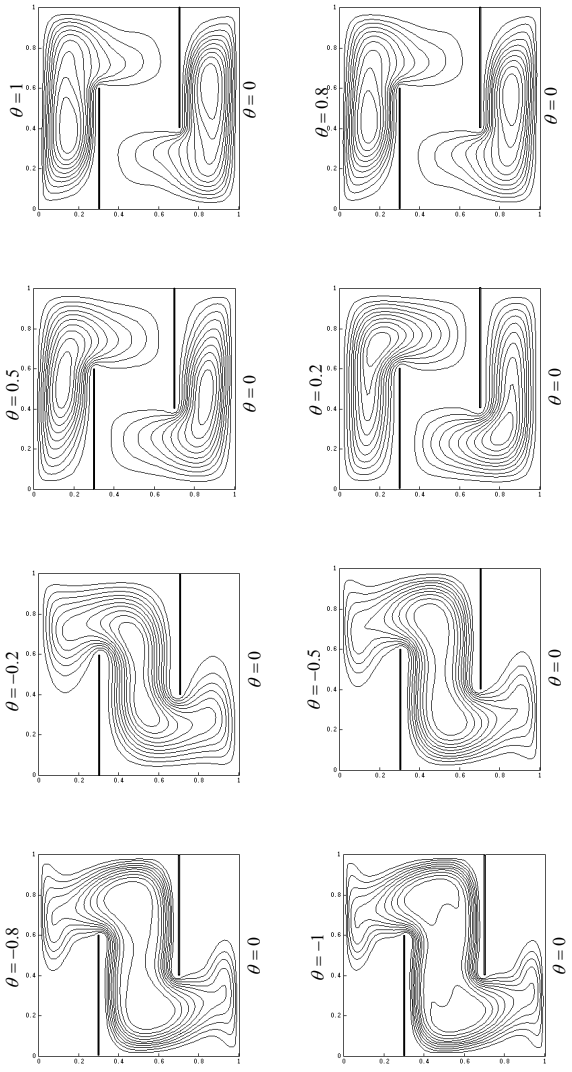

Fig. 8 Flow fields for a particular cavity with $S_b = 0.3$ and $L_b = 0.6$ when the right wall temperature was fixed at $\theta = 0$ while the left wall was varied from $\theta = 1$ to $\theta = -1$

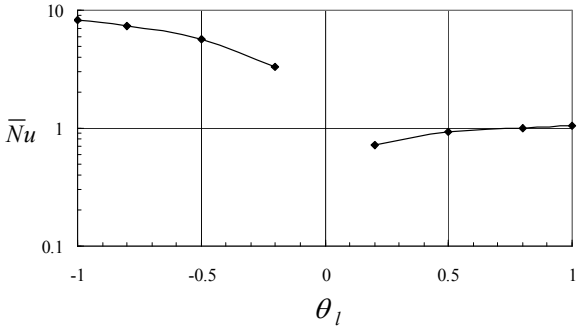

Fig. 9 Nusselt numbers for a particular cavity with $S_b = 0.3$ and $L_b = 0.6$ as a function of the left wall temperature with the right wall fixed at $\theta_r = 0$

shows that for higher Rayleigh numbers K is relatively bigger. It can be seen that the best combination of the baffle dimension and position is for baffle length $L_b = 0.7$ and its position $S_b = 0.4$. This combination gives K=7.21 at Ra=10^6, K=20.24 at Ra=10^7, and K=35.6 at Ra=10^8.

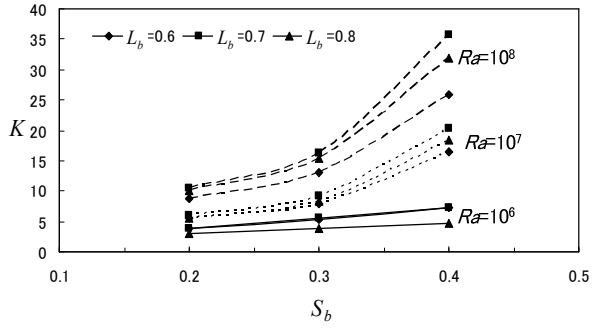

Fig. 10 *Heat flow coefficient* of the typical cavity for Rayleigh numbers Ra=10^6, Ra=10^7, and Ra=10^8

In fluids, a check valve is a mechanical device, a valve that normally allows fluid to flow through it in only one direction. Furthermore in electronics, a diode is a component that restricts the direction of movement of charge carriers. It allows an electric current to flow in one direction, but essentially blocks it in the opposite direction. Thus the diode can be thought of as an electronic version of a check valve. It was shown that the typical cavity allows the heat to flow in one direction but significantly blocks it in the opposite direction. Since the typical cavity acts like a check valve or a diode it will be referred to as a heat version of a diode. We are convinced that the characteristics of the cavity as a heat version of a diode will be significantly affected by the aspect ratio of the cavity. However in this paper only the square cavity is considered. This is because we intend to only provide the information that the cavity with baffles attached to the horizontal walls can be considered as a heat version of a diode. The full investigation of this cavity as a heat version of a diode remains to be investigated.

5 Conclusions

Heat transfer by natural convection in a differentially heated square cavity with two thin insulated baffles has been numerically studied. The cavity was performed by vertical isothermal walls and adiabatic horizontal walls. Two thin insulated baffles were attached to its horizontal walls at symmetric positions. Its non-dimensional length, L_b was varied from 0.6, 0.7, and 0.8 and its non-dimensional positions, S_b from 0.2 to 0.8. Rayleigh number ranged from 10^4 to 10^8.

The conclusions can be drawn from this study are as follows. The presence of the two baffles with non-dimensional length greater than 0.5 totally modifies the flow and temperature fields compared to the corresponding cavity without baffle. Two different flow field patterns were observed. The first pattern is flow fields with two different vortexes separated by a trapped fluid between the baffles and the second pattern is flow field with a primary vortex strangled by two trapped fluids. The flow field pattern is non-dimensional baffle positions and Rayleigh numbers dependent. For cases when $S_b < 0.5$ at low Rayleigh numbers the flow tends to circulate as a single primary vortex but at high Rayleigh numbers tends to separate into two different vortexes. For cases with $S_b > 0.5$ at low Rayleigh numbers the flow tends to separate into two different vortexes but at high Rayleigh numbers tends to circulate as a primary vortex. Nusselt number is an increasing function of Ra and a decreasing function of baffle's length. For cases when S_b <0.5, $\overline{Nu}$ is trapped fluid's dimension dependent that increases as its width increases and decreases as its length increases especially for high Ra regions. For cases when S_b>0.5, $\overline{Nu}$ is the uncovered vertical walls lengths dependent. Another interesting phenomenon of the typical cavity is that a particular case is the opposite of the other case as long as the sum of S_b is equal to 1. It was shown that the typical cavity allows the heat to flow in one direction but significantly block it in the opposite direction. Since the typical cavity acts like a check valve or a diode it will be referred to as a heat version of a diode. In order to evaluate the performance of the cavity to transfer and to block the heat flow a parameter has been promoted and named as a *heat flow coefficient*. The *heat flow coefficient* is defined as a ratio of $\overline{Nu}$ when the heat is transferred and $\overline{Nu}$ when it is blocked. The best combination of the baffle position and its length in order to block and to pass the heat flow is the particular cavity with $L_b = 0.7$ and $S_b = 0.4$.

References

[1] X. Shi and J. M. Khodadadi, "Laminar Natural Convection Heat Transfer in a Differentially Heated Square Cavity Due to a Thin Fin on the Hot Wall", *Journal of Heat Transfer*, **125** (2003), 624-634.

[2] A.Nag, A. Sarkar, and V. M.K. Sastri, "Natural Convection in a Differentially Heated Square Cavity with a Horizontal Partition Plate on the Hot Wall", *Comput. Methods Appl. Mech. Eng.*, **110** (1993), 143-156.

[3] S. H. Tasnim and M. R. Collins, "Numerical Analysis of Heat Transfer in a Square Cavity with a Baffle on the Hot Wall", *Int. Comm. Heat Mass Transfer*, **31** (2004), 639-650.

[4] F. Ampofo, "Turbulent natural convection in an air filled partitioned square cavity", *Int. J. of Heat and Fluid Flow*, **25** (2004), 103-114.

[5] S. Shakerin, M. Bohn, and R. I. Loehrke, "Natural convection in an enclosure with discrete roughness elements on a vertical heated wall", *Int. J. Heat Mass Transfer*, **31** (1988), 1423-1430.
[6] I. Sezai and A. A. Mohamad, "Suppressing free convection from a flat plate with poor conductor ribs", *Int. J. Heat and Mass Transfer*, **42** (1999), 2041-2051.
[7] E. Bilgen, "Natural convection in cavities with a thin fin on the hot wall", *Int. J. Heat and Mass Transfer*, **48** (2005), 3493-3505.
[8] A. Bejan, "Natural Convection Heat Transfer in a Porous Layer with Internal Flow Obstructions", *Int. J. Heat Mass Transfer*, **26** (1983), 815-822.
[9] R. L. Frederick, "Natural convection in an inclined square enclosure with a partition attached to its cold wall", *Int. J. Heat Mass Transfer*, **32** (1989), 87-94.
[10] Y. Yamaguchi and Y. Asako, "Effect of Partitions Wall on Natural Convection Heat Transfer in a Vertical Air Layer", *Journal of Heat Transfer*, **123** (2001), 441-449.
[11] G. N. Facas, "Natural Convection in a Cavity with Fins Attached to both Vertical Walls", *J. Thermophys. Heat Transfer*, **7** (1993), 555-560.
[12] K. Hanjalic, S. Kenjeres and F. Durst, "Natural convection in partitioned two-dimensional enclosures at higher Rayleigh numbers", *Int. J. Heat and Mass Transfer*, **39** (1996), 1407-1427.
[13] P. Joubert, P. Le Quere, C. Beghein, B. Collignan, S. Couturier, S. Glockner, D. Groleau, P. Lubin, M. Musy, A. Sergent, and S. Vincent, "A numerical exercise for turbulent natural convection in a two-dimensional partially partitioned cavity", *Int. J. Thermal Science*, **44 (**2005), 311-322.
[14] J. Neymark, C. R. Boardman III, A. Kirkpatrik, and R. Anderson, "High Rayleigh number natural convection in partially divided air and water filled enclosures", *Int. J. Heat Mass Transfer*, **32** (1989), 1671-1679.
[15] S. M. Bajorek and J. R. Lloyd, "Experimental Investigation of Natural Convection in Partitioned Enclosures", *Journal of Heat Transfer*, **104** (1982), 527-532.
[16] R. Jetli, S. Acharya, and E. Zimmerman, "Influence of Baffle Location on Natural Convection in a Partially Divided Enclosure", *Numerical Heat Transfer*, **10** (1986), 521-536
[17] E. Bilgen, "Natural convection in enclosures with partial partitions", *Renewable Energy*, **26** (2002), 257-270.
[18] G.d.V. Davis, "Natural Convection of Air in a Square Cavity; A Bench Mark Numerical Solution", *Int. J. Numerical Methods in Fluids*, **3** (1983), 249-264.
[19] M. Hortmann, M. Peric, and G. Scheuerer, "Volume Multigrid Prediction of Laminar Natural Convection; Bench-Mark Solutions", *Int. J. Numerical Methods in Fluids*, **11** (1990), 187-207.
[20] T. Saitoh and K. Hirose, "High Accuracy Bench Mark Solutions to Natural Convection in a Square Cavity", *Comput. Mech*., **4** (1989), 417-427.
[21] S.V. Patankar, Numerical Heat Transfer and Fluid Flow, Hemisphere, Washington, DC, (1980).
[22] A. Bejan, Convection Heat Transfer, John Wiley &Sons, Inc, (1999).